ISMER: A Novel Frequency Attenuated Mechanical Metamaterial for High-Magnitude Earthquake Dampening at a Cost-Effective Approach

Suraj Reddy[1]
Charter School of Wilmington[1]

Regeneron STS Report 2023-2024

Author Note/Acknowledgments

The author declares no competing monetary interests in this study. I want to acknowledge my mentor Mr. Katz at the Charter School of Wilmington and the University of Delaware's Mechanical Engineering Department zLab and Center for Composite Materials for their aid in providing experimental resources.

Abstract

Materials with unique geometrically designed microstructures, metamaterials, have gained significant attention worldwide due to their unique mechanical properties. The ability to alter the internal geometry of almost any material to increase strength exponentially is enticing due to the feasibility and possibilities of billions of designs that can change the entire scope of how a material behaves. However, mechanical metamaterials have yet to be majorly implemented at a large scale to solve crucial problems. Today's foremost problem is producing robust and efficient construction materials to prevent structural disasters such as earthquake collapses while maintaining scalability and cost-effectiveness for earthquake-prone regions such as Syria, Turkey, and Morocco. This is where ISMER (Internal Structural Modification for Earthquake Resistance), a novel metamaterial design, finds its place in low-cost earthquake resistance. Convergent Finite Element Analysis software was used to design and simulate the behavior of a special class of mechanical metamaterials under randomized seismic loading and 3D printing techniques to test the physical specimens under seismic loading. Afterward, scaled models and nanoscale mechanics were explored with Scanning Electron Microscopy (SEM), and ISMER was improved in magnitude resistance by investigating the interface's failure mechanics. Within the methods of this study, eight modular varieties, 2 to 16 units, were considered, as the structure transitions from an hourglass to a honeycomb structure as distance increases, with 8 units being perfectly vertical support and the control case that would be commonly seen in unedited microstructures of steel, for example. The most optimal design of ISMER is the 16-unit case of these varieties, so further data was collected with "stacked" lattices of ISMER monomers. These designs and measurements are proportional to the specimen itself, so they can be implemented into any solid that can be viable 3D-printed. The study resulted in a rich understanding of manipulating any material's strength by manipulating the micro-scale, in which a viable model was postulated (ISMER), and prototype models were fabricated and tested. In all, it was found that the 16-unit case (honeycomb) was the most optimal for a variety of tests such as frequency attenuation and Richter scale simulations and has major potential to be feasibly implemented into the manufacturing of housing materials as it showcased resistance to earthquakes of magnitude 6 at least in its lattice form and up to a magnitude of 7.

Keywords: Earthquakes, Metamaterial, Nanotechnology, Additive Manufacturing

Problem Statement

With the proliferation of recent seismic activity and disasters involving Earthquake collapses, namely in regions with unfavorable socio-economic circumstances (Syria-Turkey 2023 & Morocco 2023), the need for extensive application-based research in material science is clear. To provide novel and scalable material methods for earthquake resistance, the synthesis of new materials is inefficient; however, the ability to structurally edit the geometry of material for earthquake resistance has yet to be explored in extensive efforts. Currently, areas such as Tokyo employ active earthquake resistance through mechanical dampening techniques; often having the entire building disconnected from the earth below. However, these again cost upwards of $51 million, an inefficient cost gap for underdeveloped areas. ISMER will seek to solve this by integrating with the pioneering field of 3D printed houses which cut many labor costs and external factors of logistics by utilizing a single chemistry for foundation pieces.

I. Introduction

Metamaterials, which are artificially engineered materials with properties not found in nature, have attracted significant attention in recent years due to their unique mechanical properties provided solely through geometric additions in microstructure [1]. One class of metamaterials that has received particular attention is mechanical metamaterials, which can exhibit properties such as an artificial negative Poisson's ratio which can expand in the lateral direction when stretched [2]. Popular metamaterial designs utilize complex geometry which is rarely seen in nature and difficult to scale into probable alternatives. Such designs are often too complex to be considered for viable earthquake resistance techniques, as simpler designs, while perhaps not extracting the full potential of geometry, can realistically be manufactured in a timely fashion. In this study, the hourglass and honeycomb microstructure, two interconnected “shapes” often naturally present in nature, will be explored. These two specific microstructures can be transformed into each other by editing the distance between the inward point material to the center (see **Fig. 4**). This allows for the programmable auxetic structure of the materials [2][3][5]. The special negative Poisson's ratio has led to the exploration of auxetics, a term for the hour-glass structured cell but not the honeycomb, in a variety of fields, including biomedical engineering, energy storage, and tension resistance. Mechanical tension resistance is an important aspect of the mechanical behavior of mechanical metamaterials. As these materials expand in the transverse direction when stretched, they exhibit a high degree of resistance to tensile loads, which makes them highly desirable for use in applications where elevated levels of toughness and impact resistance are required [7]. Such elevated levels of toughness and impact resistance are undoubtedly present in seismic conditions, where the foundation of a building must not only cope with the weight of the building and normal force but also shear forces from the sinusoidal displacement of the ground beneath it. This warrants a deeper dive into the role of auxetic structures and their honeycomb counterparts for earthquake resistance.

The unique mechanical behavior of mechanical metamaterials under tensile loads is due to their unconventional microstructure. Typically, mechanical metamaterials are made up of a network of small, interconnected elements that can deform in such a way as to maintain their volume when subjected to tensile loads [5] [7].

In earthquake engineering, metamaterials have emerged as a promising, yet under-researched, solution to mitigate the effects of seismic waves and improve the seismic performance of structures. Seismic waves, which are generated by earthquakes, can cause considerable damage to buildings and infrastructure, resulting in loss of life and property. In 2023, earthquakes in Syria and Turkey took the lives of over 60,000 innocent people. Conventional methods of seismic protection, such as passive damping systems and seismic isolation, have limitations and can be expensive to implement. In past studies [1][5][10][15], we observed the differing methods of earthquake resistance. While base isolation allows for cost-effective and rural feasibility in its implementation, it lacks the required mechanical dampening of earthquakes. These structures are often brittle [19]. Specifically, specialized equipment such as passive dampening systems must be tailored toward larger buildings, such as skyscrapers to deal with their unique mechanical loads. Considering the wide range of expensive options, metamaterials have the potential to provide a more effective and economical solution to seismic protection. Metamaterials can be designed to exhibit negative effective mass and stiffness, making them capable of suppressing seismic waves effectively [10]. Such metamaterials would need to be implemented into the "foundation slab" of buildings, (See **Fig. 2**), as it would allow for direct dissipation of seismic energy. Utilizing this "isolated base" approach for a cost-effective approach in at-risk regions poses more promise than an entire building consisting of an ISMER lattice, as earthquake resistance often employs the *bend but doesn't break* ideology in that the foundations of structures should have mobility. However, this mobility over large timeframes can lead to inevitable growing fractures, which later in life will lead to the rapid onset of fracture. So, focussing on just the base for the first research of ISMER poses a foundational point of study.

Additionally, the current efforts in earthquake resistance involve a focus on the base of a structure. For example, high-rise buildings, often cause sedimentary displacement and are assumed to settle under their weight once the Earth below can provide balanced resistance. In the past, this approach has been modified to allow the base itself to gain frequency attenuation, effectively allowing the base of the structure itself to fluctuate while the rest of the structure can remain seemingly unharmed. However, as can be imagined, this process requires careful attention and is often only applied to expensive buildings such as skyscrapers in urban environments, leaving the rural setting unprotected. Using a similar

methodology, ISMER applies such frequency attenuation into the building materials, allowing dampening of the seismic propagation. The frequency of such seismic events and large-scale protection of major earthquakes has been shown to hover around 2-8 Hz. [14] With the higher frequency waves correlating to lower-magnitude earthquakes and the lower frequencies correlating to high-magnitude earthquakes (>6).

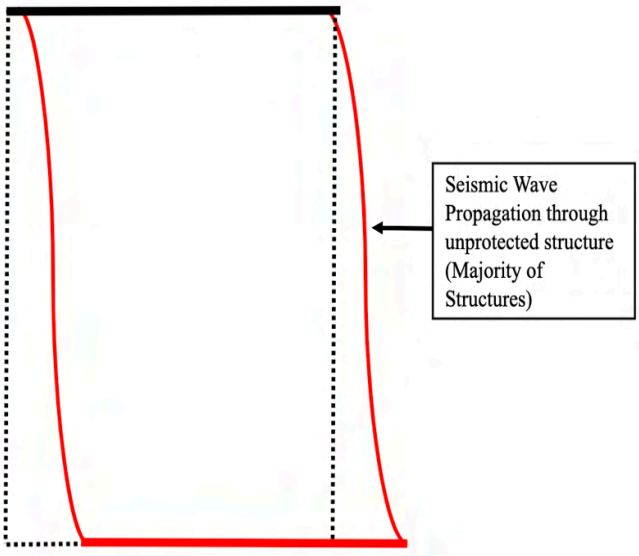

Fig. 1: Schematic of Seismic Wave Propagation in Non-reinforced Buildings [*Image created by Author]*

The application of metamaterials in earthquake engineering has the potential to revolutionize the field of seismic protection and provide a more effective and economical solution to mitigate the effects of seismic waves. ISMER seeks to provide a cost-effective solution compared to the magnitude of protection relative to the Richter scale to our battle against earthquake collapses and prospects for the use of metamaterials in earthquake engineering, making it a valuable resource for researchers, engineers, and policymakers working in this field. It should be noted that within this study, ISMER is a term for the 16-unit case of the programmable auxetic/non-auxetic structure which can be varied with the distance variable.

This study focuses on the naturally found “hourglass” shape which then transitions to a "honeycomb" structure of the supporting structures between two materials. This structure is so important due to the variability in design while maintaining the overall shape, specifically, the ability to change the distance of the inward-pointing structure from the center can influence the strength of a material. This is essential for a scalable metamaterial, as although many complex designs may exist, their modularity is questionable [5]. The hourglass structure, when faced with a tension force, allows for the inward-pointing structure to expand outwards and eventually become straightened perpendicularly to the upper and lower regions of the structure [4]. Since this inward structure is the major crux of the hourglass shape in metamaterial structures, we have hypothesized that as the distance from the center is increased, the

structure will have more earthquake resistance due to the ability of the structure to expand outwards while maintaining structural integrity under shear forces while dealing with average weight per square footage.

Due to the combination of honeycomb and hourglass lattice structures, the resulting metamaterial is theorized to have high energy absorption potential and has theoretical evidence to back that its response to seismic activity would be able to mimic the "random" vibrations of the earth from the very inside of the material, which provides a solution for the often-brittle fractures of conventional materials such as wood and steel [5] [12].

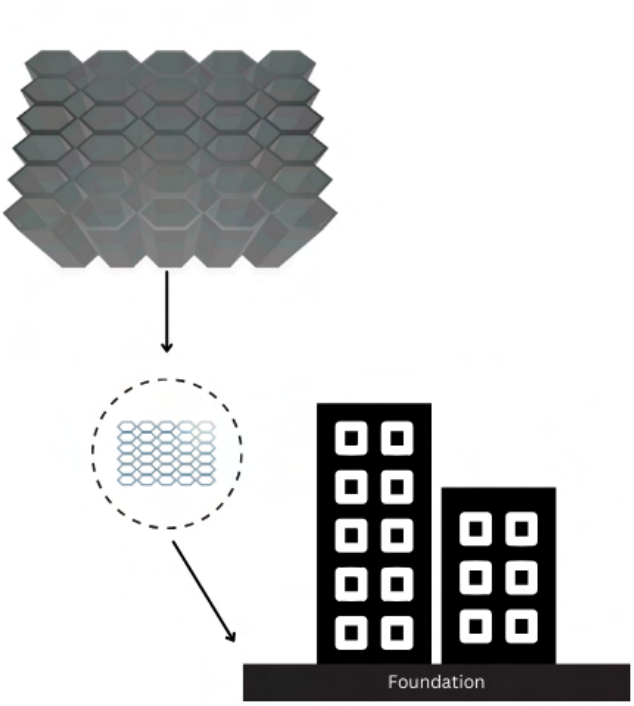

Fig. 2: ISMER Metamaterial Lattice Usage Example for High Magnitude Earthquakes in the Foundational Slab of a Structure. *Note that ISMER will be a microstructure, so millions of lattices will be present*. [*Image created by Author]*

Overall, this research aims to demonstrate the potential of auxetic programable mechanical metamaterial for use in earthquake resistance. It is widely believed that the ability to program the mechanical response of these materials, combined with their unique mechanical properties, could lead to

significant advancements in resistance technology. With the help of computational simulations and 3D printing, we can design and fabricate materials with exceptional isotropic/anisotropic properties in a direction that can aid against impact. This research aims to be a step towards the development of materials that can deform under an impact (as weight is shifted in earthquakes) but not fracture and can be returned to their original shape for large periods.

ISMER will be investigated as an alternative to these major resistance methods through a nuanced approach of computational and experimental studies as a result of initial studies finding the most optimal microstructure compared to the control case.

II. Methods

In this study, the following computational data points were collected: Stress data, Fracture data, Frequency Attenuation data, Energy dissipation data, and Richter scale failure. Experimental techniques included Finite Element Analysis seismic simulations, seismic load testing, and nanoscale mechanics.

A. Governing Equations

Eq.1 below showcases the governing equations for wave propagation in heterogeneous solids when the material is continuous and isotropic in terms of deformations. Where λ is the Lame's constants, v is the poisons ratio, and E is the Young's modulus [15].

$$\lambda = \frac{(\upsilon E)}{(1+\upsilon)(1-2\upsilon)} \quad \textbf{(1)}$$

Eq. 2 was referenced from a comprehensive study of earthquake modeling with differential equations, from which computationally convergent simulations were created. [15]

$$F_{ext} = ma = mF''(t) = -m\omega^2 F_0 cos(\omega t) \quad \textbf{(2)}$$

Utilizing Eq. 2 and Eq. 1, another model gives the ability to gain the eigenvalues after which the natural frequencies of the simulation model can be computed (Sec. III. C) [16].

$$\left(\lambda^2 \boldsymbol{I} - \boldsymbol{M}^{-1}\boldsymbol{K}\right)\boldsymbol{v} = 0 \text{ since } \upsilon \neq 0 \quad \textbf{(3)}$$

$$\det\left(\lambda^2 \boldsymbol{I} - \boldsymbol{M}^{-1}\boldsymbol{K}\right) = 0 \quad \textbf{(4)}$$

Where *M* and *K* represent the commonly utilized variables in Hooke's Law. *I* refer to the constant within Hooke's Law equation for the frequency of oscillation [16].

These equations were implemented to guide the displacement and sinusoidal nodal movement in the LS-Dyna models along with the applied seismic force constraints.

B. Computational Simulation Details

The study aimed to understand the earthquake resistance properties of programable metamaterials, meaning that they have structures with input parameters that allow for them to be altered. It should be noted that all these structures are microscopic to macroscopic structures that work in many cases,

specifically, and the entire volume of a material can be filled with these "cell"-like structures to create a lattice through computational methods. To do this, a combination of Finite Element Analysis (FEA) methods, LS-Dyna, a well-known software, was used to perform the FEA simulations. However, much of this study was from the seismic simulations produced through previously referenced literature scripting and equations. We created a script to accurately model the seismic simulations which otherwise are not available in LS-Dyna. This was a combination of Dynamic Relaxation and Elasticity modeled by *MAT_ELASTIC and *MAT_PIECEWISE_LINEAR_PLASTICITY, *BOUNDARY_PRESCRIBED_MOTION by sinusoidal displacement, *DAMPING_FREQUENCY_RANGE, and *FREQUENCY. The output requests included nodal displacements, stresses, strains, and energies. There was a fixed boundary at the top-most and bottom-most platforms of the lattice and monomer structures. The applied force is proportional to the frequency of the simulation, as referenced from **Eq. 2**. For the ISMER lattices, the applied force is proportional to the average weight/ square footage, as applying the entire force of an earthquake on a singular microstructure at the millimeter scale will result in immediate failure, so a scaled-down approach is utilized. Notably, as the lattice size increases, the proportional force for each frequency between 2 Hz - 8 Hz is increased based on the 80,000 lbs and ~2,000 sq. Ft of area in an average American home. The material utilized in the computational part of the study was 4340 steel (Alloy Steel) in LS-Dyna. Additionally, frequency and Richter scale maximum magnitude of failure data were taken from the same seismic simulations. Essentially, all computational data is from these seismic simulations aforementioned in LS-Dyna.

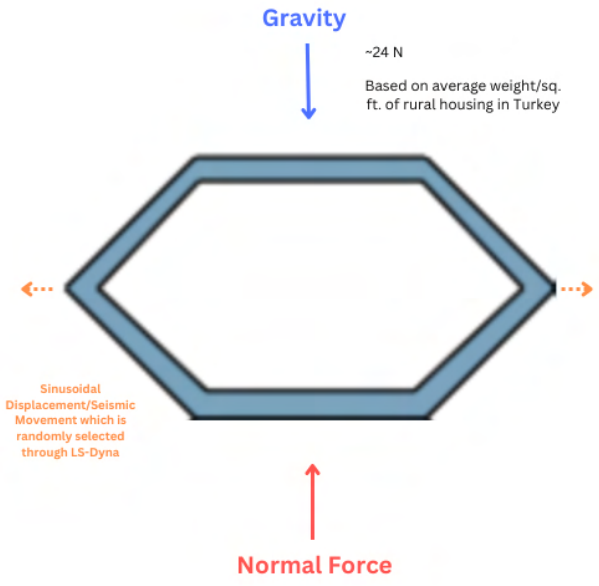

Fig. 3: Force Schematic of LS-Dyna Seismic Simulations which correspond to the assigned frequency [*Image created by Author]*

In **Fig. 3**, we observe the force schematic methodology of the LS-Dyna Frequency/Seismic simulations referenced from literature to provide accurate conditions in physical earthquake testing [17]. Force schematics and values were referenced from literature and the known average weight of 80,000 lbs and square footage of 2,147 feet in housing in the United States is sizably larger when compared to the force experienced by rural/smaller housing in at-risk regions [15][17].

The results of the study were analyzed by examining the stress, energy, and force of the 7 different geometric designs compared with the 1 vertical control case (see **Fig. 5d**). The analysis revealed an interesting trend in frequency attenuation as well, providing insight into the seismic resistance properties of programmable mechanical metamaterials. The mathematical models were used to analyze the stress, energy, and force of each design, providing valuable insight into the seismic resistance properties of the programmable mechanical metamaterials.

C. Experimental Tests

The material used in the experimental study was Polylactic acid (PLA), which is a well-known and widely used material in 3D printing. PLA is a biodegradable and environmentally friendly plastic made from renewable resources, making it an attractive option for this study. It is also relatively easy to use, as most 3D printers are compatible with this material. The physical specimens were fabricated using Fused Deposition Modeling (FDM) 3D printing techniques and Polylactic Acid (PLA) as the material. The samples were printed at a 50% infill density, where the auxetic/non-auxetic lattice itself was hard-coded into the microstructure of CAD models to enable 3D printers to produce the structure. This aided in weeding out any confounding variables. Later, improvements to the ISMER lattice of 16 units were focussed upon. The mechanical testing was from a mechanical shock testing instrument at the University of Delaware's zLab from Lansmont. The Center for Composite Materials aided in providing advice to continue the addition of compressive forces along with small seismic forces to the setup.

Scanning Electron Microscope

To understand the nanoscale mechanics of the frequency and compression-induced fractures of our PLA prototypes, we observed the samples under the *Phenom G2 Pro* Scanning Electron Microscope with its optical and SEM capabilities. The process of utilizing the PLA sample is detailed below. Sputter Coating of PLA Sample using Cressington Sputter Coating with Argon Pressurization at 0.08mb. Sample Stability was processed with suppressed air testing to ensure uniformity. Scanning Electron Microscope samples were loaded below 2 units (about 0.08 in) of the Flush edge of the Electron Charge Disposal Sample Holder by *Phenom.* Data collection was collected through Image analysis of Optical and SEM.

Scanning Electron Microscope (Phenom G2) utilized in the study [20].

III. Theoretical Results & Discussion

4 major data points are analyzed and discussed: Stress, Energy, Force, Frequency attenuation, and the maximum earthquake magnitude until failure. These data points will help decide which type of material configuration is best for seismic activity prevention [15][16].

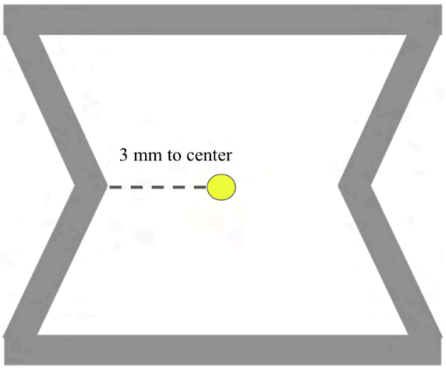

Fig. 4: Measurement example where the "3-unit" case is shown, the distance (in millimeters) is measured from the midpoint of the structural piece alone to the midpoint of the line of symmetry of the specimen. [*Image created by Author]*

A. Stress Map Analysis

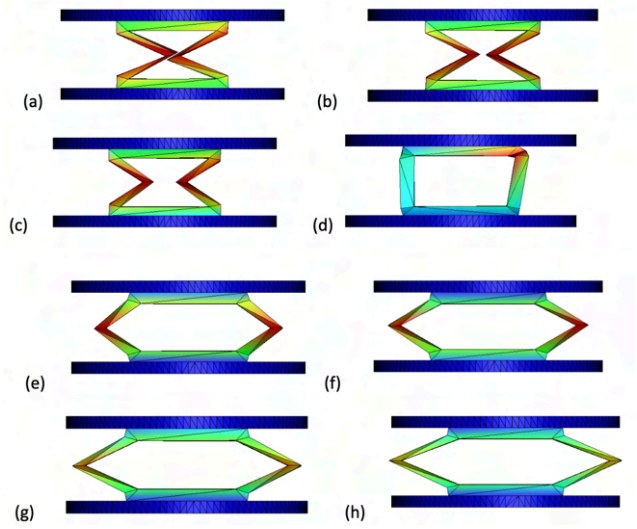

Fig. 5: 1st Principal Stress Plots of 2 units to 16 units from the Center at a common time-step of 20 milliseconds during Frequency Attenuation of 2 Hz. Note the progression of the unit cases, with the transitioning occurring in Fig. 5d at the 8-unit case. [*Image created by Author]*

As the material was compressed, the structure began to grow inwards, rather than the usual stretching outwards that materials usually undergo when they are perfectly uniform. The dark red regions indicate the 200 GPa mark, which is the Modulus of Elasticity within this case of steel. When this mark is reached, the structure fractures. All following regions down to the dark blue are indicative of 0 GPa. Additionally, it was observed that many of the structures underwent a unique process of deformation, known as necking [7]. Necking refers to a reduction in the cross-sectional area of a material, typically at a specific point along its length, under tensile loading [18]. In this case, as the structures were compressed due to the combination of shear and compressive forces of the earthquake, the structures began to buckle and collapse at their center, leading to a significant reduction in the cross-sectional area. This phenomenon is often associated with localized yielding and can have a major impact on the mechanical behavior of the material. Furthermore, the analysis revealed that the distribution of the stress and strain was not uniform throughout the structure. Instead, it was found that the stress was highest at the center, and gradually decreased towards the edges. This is because the material at the center was subjected to a higher load, due to the presence of the aforementioned sinusoidal displacement. In turn, this led to a higher strain, which increased the stress further, leading to a feedback loop of sorts.

The results in **Fig. 5** above reveal a clear trend in the material behavior when subjected to compression. The critical parts of the structure, as indicated by the high-stress regions, show a decrease as the distance from the center increases. The 8-unit case is an outlier in the study, as it only showed movement downwards and eventually buckled under 2 Hz of oscillation. Notably, the lack of movement

in the 8-unit case would understandably suffer with the addition of horizontal forces for seismic conditions, making it such that the control case would undoubtedly suffer. The tradeoff of using the 16-unit case and any case larger than 8 units is the loss of the hourglass shape, which would have provided marginally improved tension resistance. Instead, the structure would have a honeycomb geometry, which is better suited for impact based on this data.

A crucial finding from the study is that the 16-unit case showed very minimal and almost no darker red regions, indicating that the critical point of 200 GPa Yield Strength was not passed. This implies that the structure was able to withstand a significant amount of stress without yielding, making it a strong contender for applications where earthquake resistance is a primary concern.

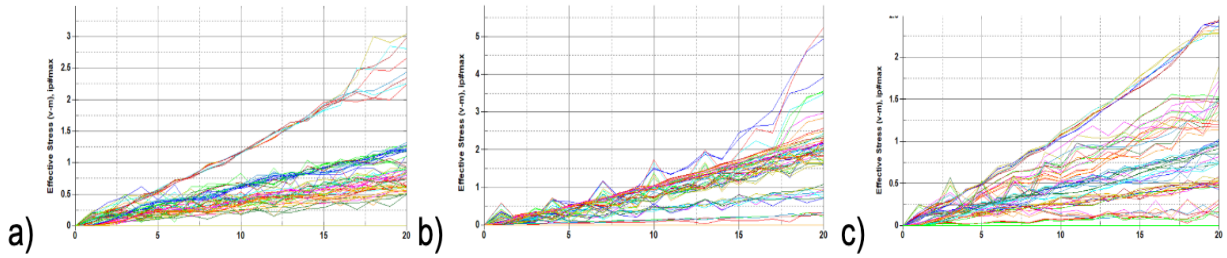

Fig. 6: Effective Stress vs. Time for 2, 8, and 16 unit cases. [*Image created by Author]*

In **Fig. 6**, intriguing results are shown in graphical data on the Effective Stress vs. Time over the major intervals in the work, 2-unit, 8-unit, and 16-unit. While there is no initially identifiable trend, stress values from over 1,000 nodes have been identified, with many of the 1,000 nodes being in regions of smaller rates of change. In **6a** and **6b**, an identifiable trend line for the regions of the "hourglass"/ "honeycomb" structure is seen, specifically in the two cases of the extremity: 2-unit and 16-unit. However, observing closely, it is paramount to understand that the 8-unit case has much larger effective stress values in general, as there is a maximum of 5 v-m for the 8-unit case while there is merely a 2.5 v-m maximum for the 16-unit case, effectively halving the stress present. This shows that the 8-unit case constitutes a large amount of stress, while also having the stress concentrated through the material, rather than in the geometric structure. This eventually led to the failure of the 8-unit case prematurely, showcasing it as a non-ideal long-term impact resistance structure, but aided by the energy analysis, the 8-unit case can fracture easily while absorbing larger amounts of energy.

In conclusion, the results of this section provide valuable insights into the behavior of materials under 2 Hz (High magnitude earthquakes) of oscillation and highlight the importance of considering multiple properties when evaluating impact resistance. Further research could be conducted to further

optimize the material and its properties for specific applications. It should be noted that the 2 Hz eigenfrequency of oscillation relates to larger earthquake magnitudes of around 6 on the Richter Scale.

B. Energy & Force Dampening

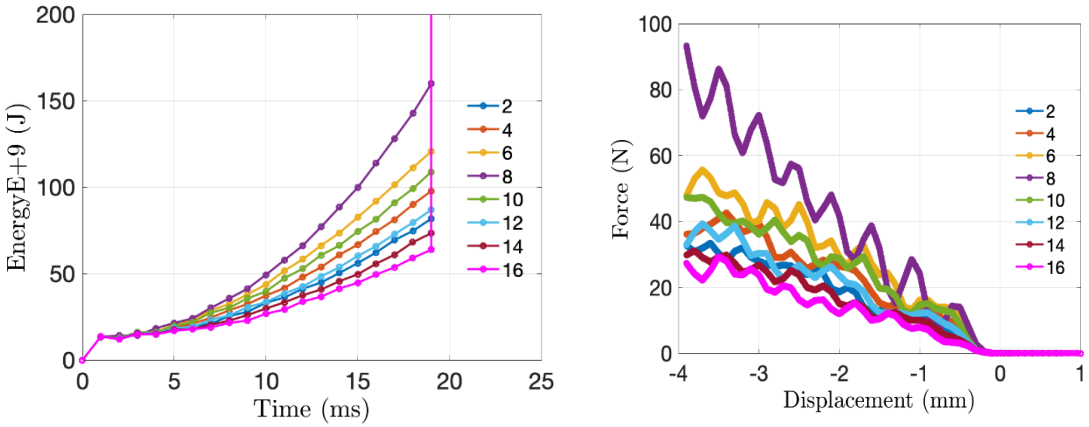

Fig. 7: a) Energy Absorption vs Time **b)** Internal force dampening response vs z-displacement of material in the Z direction. [*Image created by Author]*

For earthquake resistance, it is important to consider the mechanical properties of a material, including its ability to absorb energy as it deforms. The amount of energy a material can absorb is related to its ability to withstand impact or shock loads, and it is a key consideration in determining the suitability of a material for a particular application. However, it is important to understand that for earthquake-resistant material, energy absorption is a complex topic. Absorption should be present to an extent, however, while the maximum amount of energy absorption is great for automobile crashes, Earthquake-resistant materials cannot fracture as easily as materials used in modern automobiles. In the study we are discussing, it is observed in **Fig 7a** that the 8-unit case has the highest rate of energy growth over the same period as the other cases. This would indicate that the 8-unit case is better suited for applications that require high-impact resistance where the material itself does not need to survive. This is because the material can absorb more energy as it deforms, which enables it to fracture under stress.

However, the 16-unit case, with a lower rate of energy growth, can return to its initial condition, which suggests that it is better suited for applications where dimensional stability is important. This presents a tradeoff, as the amount of energy that can be absorbed is a tradeoff with the ability to return to the initial state. This tradeoff is particularly important for applications in earthquake resistance, where endurance is a crucial consideration [14][16]. For these applications, it is more desirable for the material to have a lower rate of energy growth, to ensure that it can maintain its shape over a longer period of load from earthquakes. The balance between energy absorption and dimensional stability is an important

consideration in material science, and the choice of material will depend on the specific requirements of the application.

The 8-unit case, as previously mentioned, is an outlier among the cases studied in this research. Despite having the highest resistance to impact as seen by its high rate of energy growth over time, it eventually buckles under load and deforms to a state where the structure indicates that failure has occurred. When looking at the other cases, the 16-unit case presents the best combination of resistive force **(Fig. 7b**), stress intensity, and energy absorption. The results for the cases between 4-14 units show minimal variation, indicating that within that range, there is not much difference in terms of these factors. It is important to note that while the 16-unit case has the lowest stress intensity, it also has the lowest energy growth rate, which can make it less suitable for applications where impact resistance is a primary concern [15]. The 8-unit case presents a tradeoff in this situation, as while it has the highest resistance to impact, it also deforms in a manner that could potentially lead to failure. When considering the other cases, the 6-unit case initially presents the best balance of resistance to impact and stability, making it the optimal choice in terms of these factors. It is important to keep in mind that this data is over a short period, so longer simulations would be required for long-term stability. On the other hand, it is important to note that the 16-unit case presents a different tradeoff. While it may not have the optimal force and energy absorption compared to the 6-unit case, the fact that it does not undergo excessive deformation under impact (see **Fig.** 5) and returns to its original shape is a valuable attribute for certain applications. This is particularly important for materials that are used in seismic metamaterials for earthquakes, as they require a high level of dimensional stability and endurance under loads over time and if the 6-unit case is not presenting this in a short period, it is not as optimal as possible. Notably, this would mean that overall, the 16-unit case has shown a greater aptitude for earthquake resistance when compared with the control and 6-unit cases.

C. Frequency Attenuation

(*Note that the following results are for a 6 x 5 monomer lattice)*

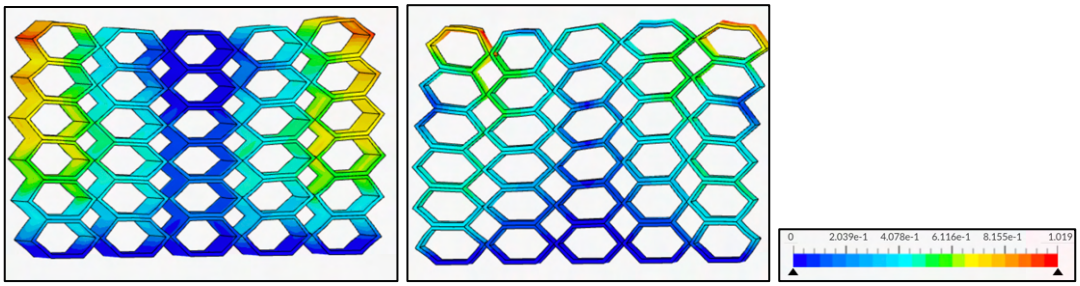

Fig. 8: a) Average over 50 continuous deformation trials: Eigenfrequency 8 Hz Displacement Solution Field **b) Average over 50 continuous deformation trials:** Eigenfrequency 2 Hz Displacement Solution Field. [*Image created by Author]*

Considering the lattice structure of the optimal 16-unit ISMER configuration, we conducted frequency attenuation. During earthquakes and intense magnitude seismic activity, there exists a crucial function of classical mechanics through Oscillatory motion. Specifically, the ability of the ISMER lattice to retain its configuration while also undergoing slight deformations under a 2 Hz and 8 Hz eigenfrequency is shown in **Fig. 8.** In **Fig. 8a** we observe non-critical displacement at the 8 Hz frequency, corresponding to smaller magnitude earthquakes (<4-5 on the Richter Scale). [14] Meanwhile, in **Fig. 8b,** we observe a similar trend across the 2 Hz frequency, which often corresponds to higher magnitude earthquakes (>6 on the Richter Scale). Specifically, in the 2 Hz case, we observe a larger amount of visible deformation in the lattice structure; we observe that its structure is still intact (has not failed) after over 50 trials of deformation at the 2 Hz frequency. The solution map details the displacement intensity, through which we see ISMER's ability to resist brittle failure while also maintaining minimal displacement. This is all while being able to attenuate the frequency of the seismic activity. This lattice structure would be the practical application of the singular lattice structure shown previously.

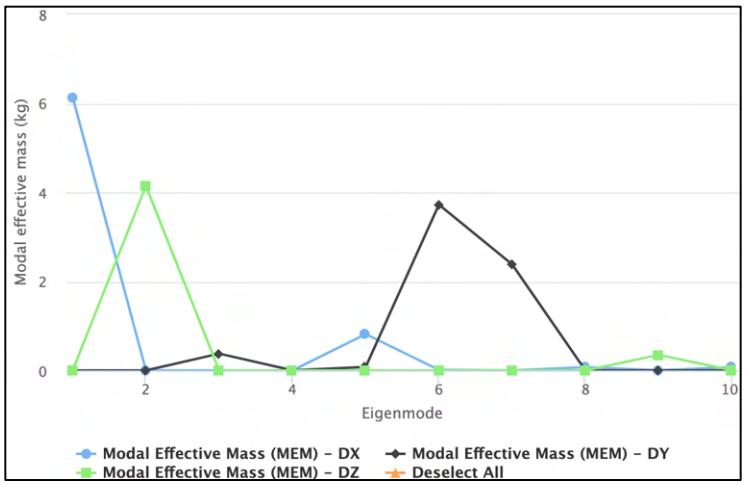

Fig. 8: c) Eigenmode vs. Model effective mass graph through 3-dimensional space. [*Image created by Author]*

In **Fig. 8c**, we see how as the Eigenmode values increase to the higher frequency values, the Z-directional MEM converges to 0. The MEM is a measure of the excitement of a structure during frequency attenuation, with larger values incurring sizable deformation and premature failure of the structure. Promisingly, we observe an interrelated trend to the previous results in which frequency attenuation is an ability of ISMER, in which the MEM values are all within acceptable ranges [13][15].

D. Earthquake Magnitude Comparison

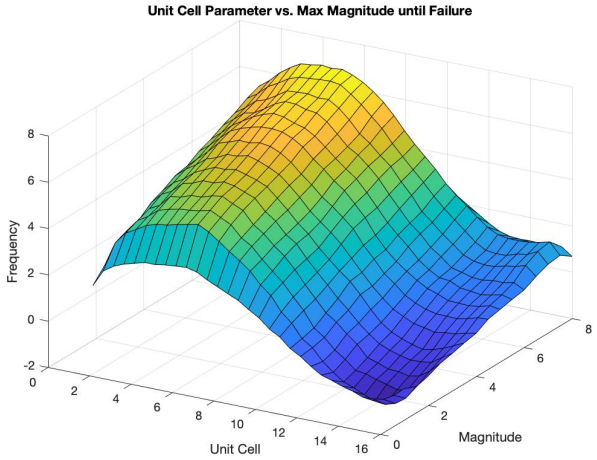

Fig. 9a: 3D plot of unit-cell dependent max-magnitude of resistance before failure and corresponding eigenfrequency. [*Image created by Author]*

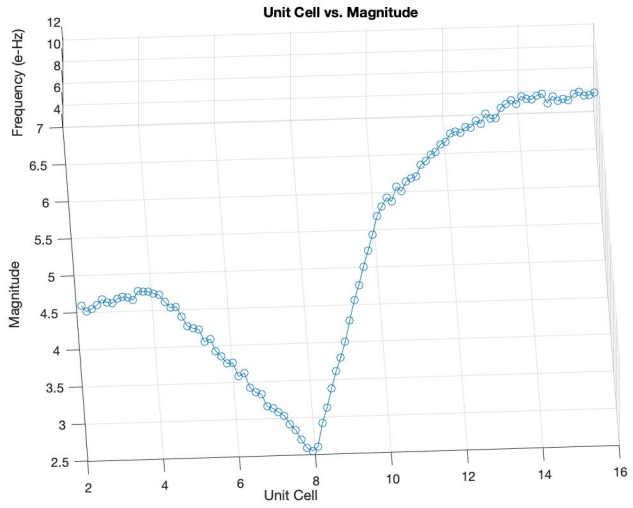

Fig. 9b: 2D representation of Unit Cell vs. Richter-Scale Magnitude Failure of all unit cell cases in lattices and those in-between from anticipatory simulations driven through ML. [*Image created by Author]*

From both **Fig. 9a & 9b**, we observe an interesting trend which will later be upheld in terms of general strength in our experiment. Originally, the hourglass auxetic structure showcases a seismic-load resistance of ~4.5 magnitude on the Richter scale. Afterward, there is a subtly increase in the magnitude of resistance in **Fig. 9b** before the unit-cell converges upon itself and leads to an eventual "failure case" at

the 8-unit cell mark. This represents the 2.5 magnitude on the Richter Scale, as the 8-unit case is again the vertical support that was expected to struggle under the shear load of earthquakes. The 4-unit case seems to be a peak in terms of the hourglass auxetic structure, whilst in earlier sections, it was shown that the 6-unit case may have been the most dampening efficient. This can be attributed to the shear load at different frequencies, which then corresponds to differing magnitudes. Afterward, we see a characteristic trend as the hourglass structures consistently improve in their magnitude of resistance.

In conclusion, the 16-unit case is observably the most computationally optimal case for earthquake resistance with its desirable mechanical properties as showcased by durability and frequency attenuation. This 16-unit case is now termed ISMER, the lattice structure which has a least 6 magnitude resistance up to 7 magnitudes.

IV. Experimental Results & Discussion: Continuum

As a preface, it should be known that the experimental study was conducted using PLA, a material often used primarily for prototyping, so failure at relatively low weightage points should be expected. The main aspect here is how the specimen will act on the previously observed computational trends. Overall, the results align with the computational ones in terms of failure prediction.

Fig. 10: 3D printed prototypes of structures scaled up by 200 percent [*Image created by Author]*

In this study, the benchmark results of 3D printed structures were analyzed and tested for their fracture threshold. To simulate seismic conditions as best as possible, weightage was used in which the weight (N) was applied 75% in the z-direction and 25% of it was oscillated in the horizontal direction by a custom testing unit. Such testing units were sourced from the Mechanical Testing Shock Tests and customized within the University of Delaware. The 3D printing aspect of the study was conducted to observe the feasibility of printing parts with varying diameters, ranging from 2 millimeters (about 0.08 in) to 16 millimeters (about 0.63 in). The results of the testing showed that the 16-millimeter structure was highly deformable and was able to return to its original position under 117.6 N of weightage, while the 8-millimeter structure showed off-trend resistance to deformation and buckling, absorbing a large amount of energy in the 78.4 N case. This is because the 8-millimeter

case is not exactly an auxetic material, so it is subject to little elasticity in its moment when being compressed.

Weight (N)	2 mm	4 mm	6 mm	8 mm	10 mm	12 mm	14 mm	16 mm
19.6	1	1	1	1	1	1	1	1
39.2	0	1	1	1	1	1	1	1
58.8	0	0	1	1	1	1	1	1
78.4	0	0	0	1	1	1	1	1
98.0	0	0	0	0	0	1	1	1
117.6	0	0	0	0	0	0	1	1

0 = Failure — 1 = No-Failure

Fig. 11: Critical Lateral Load Limit of Weak-PLA Samples of 200% Experimental Models [*Image created by Author]*

In **Fig. 11**, the results of the PLA loading studies are showcased. Please note the low Weight (N) values due to the usage of a single lattice structure and a weaker material in PLA. Through these results, it is clear there is a noticeable trend through which the 16-mm case produces the best deformability over larger weights versus others. The criteria for 1=No-Failure include the ability to not only withstand the initial load but to be able to deform and return to its original position. With the nature of the 16-mm case, it is already known to be a framework with plasticity.

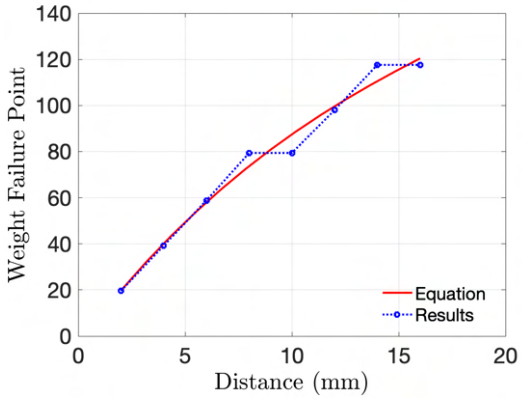

Fig. 12: Scatterplot Fit graphed along with data from the testing [*Image created by Author]*

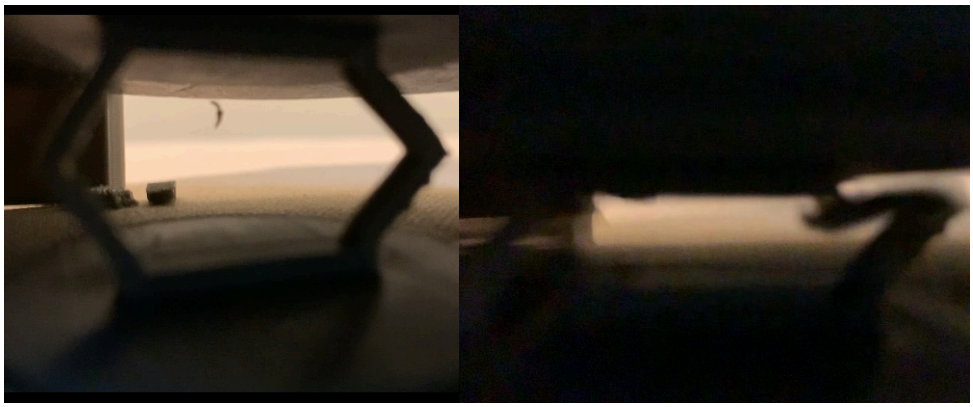

Fig. 13: 1-hour failure of the 12mm (about 0.47 in) case. [*Image created by Author]*

In **Fig. 13**, a 1-hour failure occurrence of the 12-mm case was provided. Through this, we can observe how failure often occurs at the inflection points of the structure, meaning the very ends of the outwards pointing structures that produce the honeycomb geometry. Also, observe how the interface between the honeycomb geometry and the circular surfaces is also a contingent point of failure. This opportunity to observe the continual degradation of the ISMER lattice with seismic forces finally allowed for durability testing; however, it must be noted that due to the usage of PLA, shorter times should be expected. These

V. Experimental Results & Discussion: Nanoscale

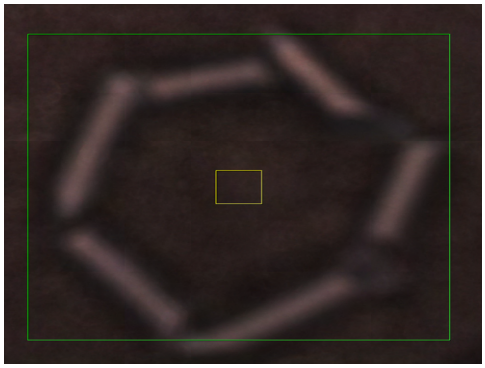

Fig. 14: 3-micrometer sample of specific 12-unit meta structure after fracture from critical lateral load limit. [*Image created by Author]*

With the scanning electron microscope (SEM), we observed the microscale of the samples and lattice structures. Due to the fact we implemented the hexagonal infill density pattern within our additively manufactured prototypes of ISMER, we were fortunate to observe the existence of such hexagonal structures in the infill pattern. The practice of additive manufacturing often incurs the construction of uneven structures even while the program indicates symmetry. Because of this, we can see how **Fig. 14** is uneven and has various defects. This is due to the 3D printing on the prototyping Ender-3, which is often utilized for initial products. In the future, a more accurate custom printer will be developed.

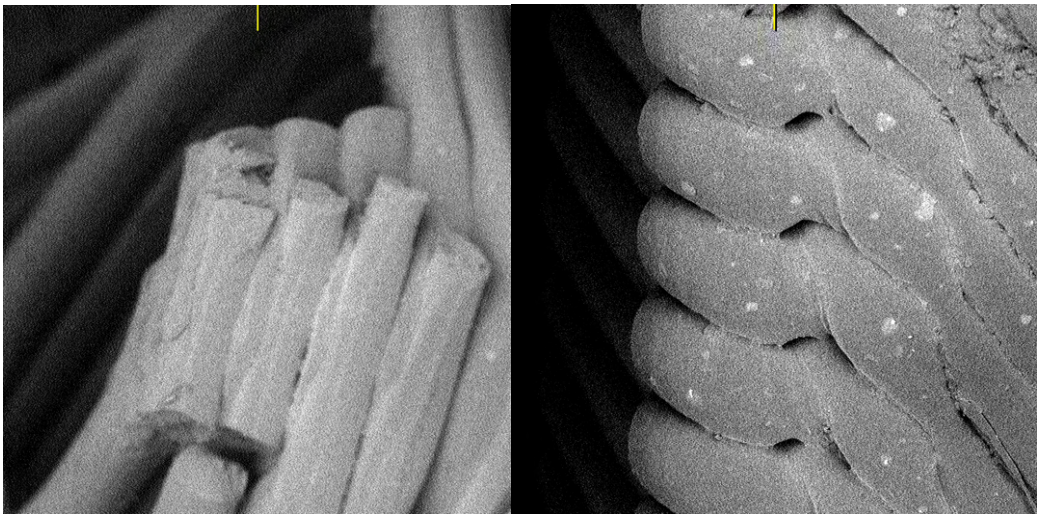

Fig. 15: **a)** Failure at 2 Hz in the interface of structure and surface additively manufacturing 8-unit case **b)** 16-unit case through which the structure is intact at the interface of the structure and surface. [*Image created by Author]*

As indicated in **Fig. 15**, the SEM captured the microscale of the post-testing environments of the 8-unit vs 16-unit case. The 8-unit case is known to be the naturally occurring support in materials, through which vertical "supports" work to upholster the material. However, we observe here how there was a dramatic failure in the specimen. Compared to the 16-unit case, which stayed intact at the 2 Hz eigenfrequency, the 8-unit case showcases the separation of layers within the 3D space. Not only is there segmentation of the layers, but the process of delamination of the fibrous layers is also present, indicating the additive manufacturing implications of ISMER. Because of this, adhesive agents such as (3-GLYCIDOXYPROPYL) TRIMETHOXYSILANE may be utilized in the manufacturing process of ISMER at the large scale to include the betterment of the adhesive layer between the layers to prevent such premature failure. In the 16-unit case, we see sustainment through the 2 Hz eigenfrequency attenuation. However, notice the defects present in the sample, further indicating how the additive manufacturing process must be refined to produce reliable prototypes and production of ISMER.

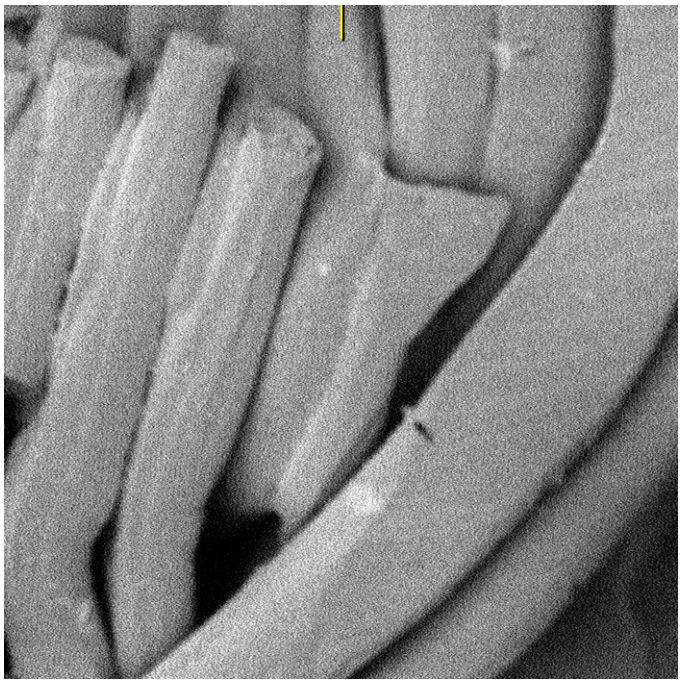

Fig. 16: Delamination of the 8-unit sample at 8 Hz. [*Image created by Author]*

In **Fig. 16**, the delamination of fiber layers of the 8-unit sample at 8 Hz is observed. Even at the 8 Hz frequency, the structure struggles to prevent failure at the interface when faced with low-magnitude earthquakes. This holds importance in realizing that the 8-unit case is the naturally occurring vertical substrate often utilized in many micro-architectural frameworks. It should be noted that this represents a 3D-printed version, meaning that the results cannot be generalized to wood and steel vertical supports. However, it is important to observe that the stress of the structure failed prematurely due to the separation of fiber layers, which was not observed in **Fig. 15b**, through which the 16-unit case produced stability under a more intensive load. Overall, we observe from the nanoscale that the 16-unit case which provides optimal frequency attenuation also holds a similar positive trend at the nanoscale. This is upheld by the fact that the delamination and fiber-matrix adhesion failure at the nanoscale of the 8-unit vertical structure showcases premature failure. The fact that the fiber-separation occurred at the interface at both 2 Hz and 8 Hz frequency representing ~4 magnitude and >6 magnitude earthquakes, respectively, showcases that in multiple ranges of the earthquakes, the vertical support is by far not optimal. With the displacement of the structure, the interface is put under extreme stress due to the shear load being applied. However, this interface displacement between the lattice structure should not realistically provide the same effect. Yet we also see the dramatic failure of the 8-unit case in the continuum experiments.

VI. Conclusions

This research report aims to provide a comprehensive overview of the state of ISMER (Internal Structural Modification for Earthquake Resistance) and its programmable state of earthquake resistance. With frequency attenuation analysis, continuum-scale experiments, followed by nanoscale separation analysis, we conclude that ISMER has showcased viable earthquake resistance in its monomer and lattice form. Firstly, we observe at the 16-unit configuration ratio, ISMER can withstand eigenfrequencies of 2 Hz - 8 Hz. This correlates to around 4-6 magnitude earthquakes, highlighting widespread protection. This finding was again upholstered through the stress and energy dampening analysis of the 16-unit case amongst the other 7 cases, through which we observed the absence of stress singularities at critical points amongst the singular lattice structure. Later, we come back to the lattice structure of the 16-unit case, through which we observed the deformability of the sample while under the intense load of numerous cycles of simulations, that the 16-unit case holds promising applications in larger-scale earthquake collapse prevention. Although defects were present in the layers, the material dependence of PLA was notable for a prototyping experiment, and in the future, we aim to utilize refined 3D printing technology and refined filaments like construction materials such as steel to produce "real-world"-ready lattice structures. Such lattice structures would be implemented in what is commonly termed the foundational slab support structure of housing. This slab is often a horizontal platform which a building rests upon. With ISMER being implemented within this slab microstructure, we have theorized that such an addition would allow for seismic resistance and prevent scenarios such as **Fig. 1.** While concrete is often utilized for these structures, the possibility of implementing steel as the foundation serves for further research. Along with this, the continuity of the slab must be researched in the future to support the defined notion of earthquake resistance. Additionally, the expected cost of foundational support with ISMER would be around $5,000 due to the lack of labor needed from the 3D printer taking care of manufacturing. However, this is still an important future exploration to consider. Not to mention, in the future, more extensive computational studies will be needed to consider the long-term durability of ISMER in the face of frequent earthquakes over periods of years. Notably, ISMER holds promise for rural feasibility due to the rapid scalability through 3D printing. Currently, ISMER holds a promising approach to earthquake resistance in areas such as Syria and Morocco for ISMER, and one in which future custom prototypes will be iterated due to their cheap implementation by just 3D printing.

Main Resistance Methods	Cost Effective	Extensive Dampening	Rural Feasibility
Foundational Strengthening	✓	✗	✓
Mechanical Dampeners	✗	✓	✗
ISMER	✓	✓	✓

Fig. 17: Future benefits of ISMER considering current study. [*Image created by Author]*

Bibliography

[1] Anna Stavitskaya, Maria Rubtsova, Aleksandr Glotov, Vladimir Vinokurov, Anna Vutolkina, Rawil Fakhrullin, and Yuri Lvov. Architectural design of core–shell nanotube systems based on aluminosilicate clay. Nanoscale Advances, 4(13):2823–2835, 2022.

[2] Daniel Acuna, Francisco Guti´errez, Rodrigo Silva, Hum- berto Palza, Alvaro S Nunez, and Gustavo Du¨ring. A three-step recipe for designing auxetic materials on demand. Co-unifications Physics, 5(1):113, 2022.

[2] Faisal Amin, Murtaza Na jabat Ali, Umar Ansari, Mariam Mir, Muhaunitad Asim Minhas, and Wakeel Shahid. Auxetic coronary stent endoprosthesis: Fabri- cation and structural analysis. Journal of Applied bioma- terials & functional materials, 13(2):127–135, 2015.

[3] Arpan Gupta, Rishabh Sharma, Aman Thakur, and Preeti Gulia. Metamaterial foundation for seismic wave attenuation for low and wide frequency band. Scientific Reports, 13(1):2293, 2023.

[4] Reza Jafari Nedoushan, Yongsan An, and Woong-Ryeol Yu. New auxetic materials with stretch-dominant architecture using simple trusses. Mechanics of Advanced Materials and Structures, pages 1–17, 2021.

[5] H MA Kolken and AA Zadpoor. Auxetic mechanical metamaterials. RSC advances, 7(9):5111–5129, 2017.

[6] Paul Mardling, Andrew Alderson, Nicola Jordan-Mahy,

and Christine Lyn Le Maitre. The use of auxetic materials in tissue engineering. Biomaterials science, 8(8):2074– 2083, 2020.

[7] Mariam Mir, Murtaza Najabat Ali, Javaria Sami, and Umar Ansari. Review of mechanics and applications of auxetic structures. Advances in Materials Science and Engineering, 2014, 2014.

[8] Xin Ren, Raj Das, Phuong Tran, Tuan Duc Ngo, and Yi Min Xie. Auxetic metamaterials and structures: a review. Smart materials and structures, 27(2):023001, 2018.

[9] Fabrizio Scarpa. Auxetic materials for bioprostheses [in the spotlight]. IEEE Signal Processing Magazine, 25(5):128–126, 2008.

[11] Hui Wan, Hideyuki Ohtaki, Shinya Kotosaka, and Guom- ing Hu. A study of negative poisson's ratios in auxetic honeycombs based on a large deflection model. European

Journal of Mechanics-A/Solids, 23(1):95–106, 2004.

[12] Yan Yao, Hao Yuan, Huiwen Huang, Jinglong Liu, Lizhen Wang, and Yubo Fan. Biomechanical design and analysis of auxetic pedicle screw to resist loosening. Computers

in Biology and Medicine, 133:104386, 2021.

[13] Wande Zhang, Pranav Soman, Kyle Meggs, Xin Qu, and Shaochen Chen. Tuning the poisson's ratio of biomaterials for investigating cellular response. Advanced functional materials, 23(25):3226–3232, 2013.

[14] Duggal, Shashikant K. Earthquake resistant design of structures. New Delhi: Oxford university press, 2007.

[15] Gupta, Arpan, et al. "Metamaterial foundation for seismic wave attenuation for low and wide frequency band." Scientific Reports 13.1 (2023): 2293.

[16] Wilkins, Chloe. "Earthquake Modelling with Differential Equations."

[17] Lindeburg, M. R., & McMullin, K. M. (2014). Seismic design of building structures: a professional's introduction to earthquake forces and design details. Professional Publications, Inc..

[18] Tu, S., Ren, X., He, J., & Zhang, Z. (2020). Stress–strain curves of metallic materials and post-necking strain hardening characterization: A review. *Fatigue & Fracture of Engineering Materials & Structures*, *43*(1), 3-19.

[19] Tse, S. T., & Rice, J. R. (1986). Crustal earthquake instability in relation to the depth variation of frictional slip properties. *Journal of Geophysical Research: Solid Earth*, *91*(B9), 9452-9472.

[20] Thermo Scientific. (n.d.). Phenom XL desktop SEM. Retrieved October 10, 2023, from https://www.nanoscience.com/products/phenom-desktop-sem/phenom-xl-desktop-sem/